

Supporting Information

Seagrass-mediated phosphorus and iron solubilisation in tropical sediments

Kasper Elgetti Brodersen^{1,2,*}, Klaus Koren^{2,*}, Maria Moßhammer^{2,*}, Peter J. Ralph¹, Michael Kühl^{1,2,#}, Jakob Santner^{3,4,#}

¹Climate Change Cluster (C3), Aquatic Processes Group, Faculty of Science, University of Technology Sydney (UTS), Sydney, Australia.

²Marine Biological Section (MBL), Microenvironmental Ecology Group, Department of Biology, University of Copenhagen, Helsingør, Denmark.

³Division of Agronomy, Department of Crop Sciences, University of Natural Resources and Life Sciences, Vienna, Austria.

⁴Rhizosphere Ecology and Biogeochemistry Group, Institute of Soil Research, Department of Forest and Soil Sciences, University of Natural Resources and Life Sciences, Vienna, Austria.

*These authors contributed equally to this work and share the first authorship of this paper.

#Corresponding authors: mkuhl@bio.ku.dk (Michael Kühl) and jakob.santner@boku.ac.at (Jakob Santner)

Running title: Seagrass nutrient mobilization

Contents: Notes S1, Figures S1-S10, 23 pages

Table of Contents

Materials and Methods.....	3
(a) List of used chemicals.....	3
Chemicals for optical sensor preparation.....	3
Chemicals and materials for preparing diffusive gradients in thin films (DGT) gels.....	3
(b) Experimental setup and sampling site	4
<i>In situ</i> measurements.....	6
(c) Optode preparation	7
(d) Planar optode calibration.....	8
(e) Luminescence imaging.....	8
(f) DGT gel preparation	9
(g) DGT gel analysis and image generation.....	11
(h) DGT interpretation	12
(i) Calibration plots.....	14
Planar optode calibrations.....	14
DGT calibrations	16
Supplementary Data.....	17
Figure S7. O ₂ distribution.....	17
Figure S8. pH heterogeneity.....	18
Figure S9. Fe(II), phosphate and pH distribution.....	19
Figure S10. Calcium distribution.....	21
References	23

MATERIALS AND METHODS

Notes S1

In the following sections, we provide detailed information about methods and materials used to obtain the chemical images and results presented in the main document.

(a) List of used chemicals

Chemicals for optical sensor preparation

Platinum(II)-meso(2,3,4,5,6-pentafluoro)phenyl-porphyrin (PtTFPP) was bought from Frontier Scientific (frontiersci.com). Macrolex® fluorescence yellow 10GN (MY) and carbon black were obtained from KREMER (kremer-pigmente.de). The lipophilic pH indicator 1-hydroxypyrene-3,6,8-tris-bis(2-ethylhexyl)sulfonamide (lipo-HPTS) was generously provided by Dr. Sergey Borisov (Graz University of Technology, Austria), who prepared it according to the literature.¹ Perylene and all organic solvents were obtained from Sigma-Aldrich (sigmaaldrich.com). The polyethylene terephthalate (PET) support foil was obtained from Goodfellow (goodfellow.com). Polyurethane hydrogel (Hydromed D4) was obtained from AdvanSource biomaterials (advbiomaterials.com). Polystyrene (PS, MW 250,000 g mol⁻¹) was bought from ACROS Organics (acros.com).

Chemicals and materials for preparing diffusive gradients in thin films (DGT) gels

Acrylamide, AgNO₃, ferrozine, KI, NaCl, MES buffer, NaNO₃, ascorbic acid, KH₂PO₄, H₂SO₄, potassium antimony tartrate, CH₃COOH and CH₃COONa were obtained from Sigma-Aldrich (sigmaaldrich.com). HNO₃, HCl, NaOH, FeSO₄, and ammonium molybdate tetrahydrate were purchased from Merck (merck.de). High-purity NaOH, ZrOCl₂ · xH₂O and AgI were bought from Alfa Aesar (alfa.com). HNO₃ was purchased from Roth and (NH₄)₂S₂O₈ (APS) as well as tetramethylethylenediamine (TEMED) were obtained from VWR (vwr.com). The DGT gel cross-linker was bought from DGT Research (dgtresearch.com). The suspended particle reagent iminodiacetic acid (SPR-IDA), a resin mainly selective for transition metal cations, was purchased from Cetac (cetac.com). All chemicals were of highest available purity and were, if not stated differently, used as received.

Membranes for DGT sampling and calibration were purchased from Whatman (Whatman Nuclepore, pore size 0.2 μm, thickness 10 μm; whatman.com) and from Tanaka Sanjiro Co Ltd. (plankton mesh DIN 100-60; mesh opening 60 μm, thickness 50 μm; www.tanaka-sanjiro.com).

(b) Experimental setup and study site

Seagrasses and carbonate-rich sediment sampling

Seagrass specimens of *Cymodocea serrulata* (R.Br.) Asch. & Magnus, and carbonate-rich, tropical marine sediment were collected from shallow coastal waters (<2 m depth) at Green Island, Cairns, Australia (16° 45' 26.244" S; 145° 58' 25.7376" E). After sampling, seagrasses and sediment were kept in constantly aerated seawater reservoirs at the Monkman Reef Research Station on Green Island before further analysis. Prior to experiments, the sediment was sieved to obtain the <1 mm grain size fraction excluding any larger infauna, while maintaining essential nutrients, buffering salts and microbes.

Experimental chambers

The experimental chambers (Fig. S1; inner dimensions 10 × 130 × 120 mm) consisted of custom-made narrow, transparent acrylic chambers with a removable back window made of polycarbonate for ease of access when transplanting the seagrasses and positioning the sensors/gels (described below). The experimental chambers were glued onto the side of aquaria in an upright position. The aquaria were made of thin glass walls (~3 mm) to improve the optical properties during imaging. The selected seagrasses were gently uprooted and transplanted into the pre-sieved/homogenized sediment that had been filled into the experimental chambers. Natural seawater from the sampling site was used throughout the experiments (temperature of ~28°C; salinity of 30).

Illumination was provided by halogen lamps (Philips Incandescent 230V PAR38 80W) illuminating the leaf canopy with a photon irradiance (PAR, 400-700nm) of ~500 $\mu\text{mol photons m}^{-2} \text{s}^{-1}$, as measured with a spherical scalar irradiance sensor (US-SQD/L, Walz GmbH, Germany) connected to a calibrated photon irradiance meter (ULM-500, Walz GmbH, Germany). The light level was mimicking natural mid-day photon irradiances at leaf canopy height of the seagrass meadow. Water-column movement and aeration were ensured via a submerged water pump and an air stone connected to an air pump, respectively.

Diffusive gradients in thin films (DGT) gels for single-analyte imaging of sulphide and phosphate distributions were positioned at the removable back-wall of the experimental chambers and were separated from the sediment/below-ground seagrass biomass by a fine mesh (plankton mesh DIN 100-60, mesh size 60 μm , thickness of 50 μm), to allow for gel deployment and sampling without disturbing the sediment. Multi-ion gels (Zr-oxide-SPR-IDA gels) were covered with a Whatman

Nucleopore membrane (pore size 0.2 μm , thickness 10 μm) and positioned in direct contact with the sediment.

Planar optical sensor foils for pH and O₂ imaging, *i.e.*, planar optodes (described below), were fixed onto the transparent aquarium wall using a thin layer of seawater, carefully avoiding air bubble formation in between the optode and the aquarium wall. Investigated seagrass specimens were positioned in the experimental chamber ensuring good contact between the below-ground biomass and the optodes or the DGT gels on the opposite side of the investigated roots, before careful addition of sieved natural marine sediment from the sampling site. This procedure enabled subsequent superimposing of the plant tissue structures onto the optode images. To precisely align the below-ground tissue with the chemical images, all obtained camera pictures included a ruler for guidance, which along with detailed root structure observations on the chemical images allowed us to precisely position the seagrass tissue on the color coded chemical images. The plant tissue structures were positioned on the chemical images using the software Inkscape (version 0.48; inkscape.org).

The seagrass specimens transplanted into experimental chambers with sieved sediment were left undisturbed for a minimum of 12 h prior to experiments to ensure establishment of steady state chemical/redox conditions. This was enabled by separating the sediment and DGT gels by an additional plastic foil, to avoid diffusion into the gels before the sediment had reached steady state chemical conditions (after \sim 5 h as determined in a pilot study), after which the plastic foil was carefully removed. Hence, two plastic foils and DGT gels were deployed in contact with each seagrass specimen and sediment (*i.e.*, in the following order: plant and sediment, fine mesh, plastic foil 1, DGT 1 (*e.g.* for light measurements), plastic foil 2, DGT 2 (*e.g.* for dark measurements)), thus enabling steady-state DGT measurements in darkness and light without disturbing the sediment during retrieval. This did not account for the multi-ion gels as they were first covered with a Whatman Nuclepore membrane and then positioned in direct contact with the sediment, in a chamber not containing the fine plankton mesh, for 24 h to ensure sufficient analyte accumulation for the subsequent analysis. This procedure was chosen as the restricted spatial dimensions of the multi-ion gels (\sim 3x5 cm) did not allow for retrieving the gels and/or the additional plastic foil without opening the experimental chamber.

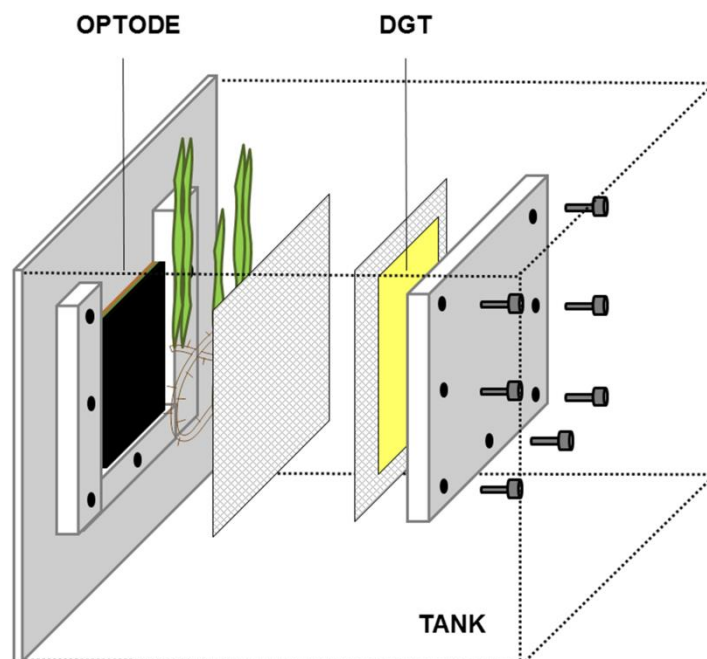


Figure S1. Schematic drawing of the custom-made, narrow experimental chamber positioned within a 20 L seawater reservoir. Note the position of the optode and DGT gels on opposite sides of the investigated roots. During measurements, we carefully ensured good contact between the below-ground biomass with the optode or the DGT gels, respectively.

Seagrass photosynthetic performance during cultivation

We assessed the photosynthetic competence of the investigated seagrasses using fiber-optic pulse amplitude modulated (PAM) chlorophyll fluorometry (JuniorPAM, Walz GmbH, Germany) measuring the maximum quantum yield of photosystem II (PSII) activity in the dark adapted state ($F_v/F_m =$ the maximal quantum yield of PSII).² The F_v/F_m of all investigated seagrasses remained >0.7 throughout the experiments, confirming that the seagrasses were photosynthetically competent during cultivation (data not shown).

In situ measurements

In situ measurements of the natural dynamics and concentrations of sulphide within the investigated seagrass meadow were obtained by deploying sulphide sensitive AgI DGT gels mounted within commercial DGT samplers (DGT Research Ltd., www.dgtresearch.com) in the sediment over diurnal cycles (Fig. S2). For day-time sulphide measurements, the DGT gel probes were deployed in the seagrass meadow at sunrise and retrieved at sunset, and vice versa for the night-time sulphide measurements, *i.e.*, a sulphide exposure period of ~ 12 h for both day- and night-time deployments.



Figure S2. Deployment of sulphide sensitive DGT gels *in situ*. (a) The sulphide sensitive DGT gels were mounted in DGT samplers. (b) The study site within the seagrass meadow (Green Island, Cairns, Australia). (c) DGT gel deployment. (d) Gel sampler positioned within the seagrass meadow. To enable DGT deployment, a less densely vegetated spot was selected within the dense multi-species seagrass meadow. The DGTs were deployed at sunrise and retrieved at sunset for the daytime measurements and *vice versa* for the night measurements. Two deployments were performed in the investigated seagrass meadow.

(c) Optode preparation

Planar optical sensor films, *i.e.*, planar optodes, were prepared via knife-coating a sensor cocktail onto a transparent PET foil as follows. The cocktail used for the O₂ optode consisted of 1.5 mg of MY, 1.5 mg of PtTFPP, 100 mg of PS and 1 g of CHCl₃. After all components were dissolved in CHCl₃, the solution was spread on a dust-free PET foil using a film applicator (byk.com) to yield a ~10 µm thick sensor film after solvent evaporation. In order to exclude background light and to achieve highest possible resolution, an optical isolation layer was coated on top of the sensor film. This layer

consisted of 1% w/w (10 mg) of carbon black dispersed in 1 g 10% w/w solution of D4 (EtOH: water, 9:1 w/w) and was knife-coated on top of the sensor film with a final thickness of the isolation layer of $\sim 7.5 \mu\text{m}$.

The applied pH optode was prepared by knife coating a sensor cocktail consisting of 1 mg lipo-HPTS, 1 mg perylene and 100 mg D4 dissolved in 1 g of THF on a dust-free PET support foil. After solvent evaporation, the sensor layer had a thickness of $\sim 10 \mu\text{m}$. For the pH optode, we decided not to use an isolation layer as migration of the indicator dye into this layer is more likely than in case of the O_2 optode. This resulted in a slightly reduced spatial resolution owing to light scattering from the sediment.

(d) Planar optode calibration

A calibration curve for the planar O_2 optode was generated as follows. A small piece of O_2 optode was taped into the experimental chamber. Oxygen levels of the seawater within the chamber were altered by means of compressed air and nitrogen, which were mixed by a computer-controlled gas mixer (SensorSense, The Netherlands). Simultaneously, the O_2 level in the water column was monitored via a calibrated O_2 optode system, *i.e.*, an O_2 optode probe connected to a fiber-optic O_2 meter (Piccolo2, PyroScience GmbH, Aachen, Germany). To ensure that equilibrium was reached, each calibration step was held for a minimum of 20 min. The final calibration was obtained by relating the extracted red/green image ratios to the measured O_2 levels. The calibration curve for the planar pH optode was generated by exposing the pH optode to buffer solutions with known pH (pH of 5.3, 6.7, 7.2, 7.6, 8.1, 9.1 and 12) as measured using a calibrated pH microelectrode (Unisense A/S, Aarhus, Denmark). The salinity was adjusted to 30 using NaCl and was checked using a calibrated refractometer.

(e) Luminescence imaging

A ratiometric RGB camera setup was used for O_2 imaging³ with a SLR camera (EOS 1000D, Canon, Japan) combined with a macro objective lens (Macro 100 f2,8 D, Tokina, Japan), a 530 nm long-pass filter (Uqgoptics.com), and an additional plastic filter (#10 medium yellow; leefilters.com) positioned in front of the long-pass filter to reduce the background fluorescence. A 455 nm multichip LED (LedEngin Inc, RS Components Ltd, Corby, UK) combined with a bandpass filter was used for excitation of the O_2 planar optode; the LED was powered by a USB-controlled LED driver unit (imaging.fish-n-chips.de). Image acquisition and control of the SLR and LED were achieved with the software look@RGB (imaging.fish-n-chips.de).

A similar ratiometric approach was chosen for pH imaging,⁴ using a 2CCD multispectral camera (JAI AD-080 GE; jai.com) equipped with a video objective lens (1.4/23 CCTV-LENS 400 - 1000 nm; schneiderkreuznach.com) mounted with a 460 nm long-pass filter (schneiderkreuznach.com) and an additional plastic filter (#10 medium yellow; leefilters.com). The pH planar optode was excited with a high-power 405 nm LED (LedEngin; rs-online.com) with a custom-built LED trigger (National instruments USB 6008). Image acquisition and triggering of the LED was done via custom-made software (bioras.com).

Acquired RGB color images were split into red, green, and blue channels and analyzed using the software ImageJ (rsbweb.nih.gov/ij/). For O₂ concentration images, the red channel (O₂ sensitive emission of the indicator dye) and green channel (emission of the inert reference dye) of the color images were divided using the ImageJ plugin Ratio Plus (ratio = red/green). Afterwards, the obtained ratio image was fitted to a previously obtained calibration curve (Fig. S3 and S4) using the Curve Fitting tool of ImageJ (exponential decay function). For pH images, the red channel (pH sensitive emission of the indicator dye) and the blue channel (emission of the reference dye) of the images were divided using the ImageJ plugin Ratio Plus (ratio = red/blue). Subsequently, the obtained ratio image was fitted with a previously obtained calibration (Fig. S3 and S4) using a linear fit within the boundaries (pK_a ± 1 pH units). Calibrated O₂ concentration and pH images were further analyzed in ImageJ.

(f) DGT gel preparation

Polyacrylamide diffusive gel preparation. The polyacrylamide DGT gels were prepared from a stock gel solution, according to standard procedures.⁵ The stock solution was produced by adding 15 mL DGT gel cross-linker to 47.5 mL MilliQ water (resistivity: >14.1 MΩ cm⁻¹), before adding 37.5 mL acrylamide solution (40% w/w). The mixture was stirred and then stored at 4°C. Acid-washed glass plates were separated by a spacer (either 0.25 mm or 0.50 mm) and clipped together. The gel solution (2 mL) was mixed with 14 μL APS solution (10% w/w) and 5 μL TEMED and quickly pipetted between the glass plates. The plates were placed for polymerization in an oven at 42°C for 40 minutes. Subsequently, the polyacrylamide hydrogels were soaked in MilliQ water for 24 hours (the water was exchanged at least three times) and were then stored in a 0.03 M NaNO₃ solution prior to further use.

Precipitated Zr-oxide binding gel for densitometric phosphate mapping. The phosphate binding gel was prepared by soaking a 0.4 mm thick diffusive gel in a ZrOCl₂ solution according to Guan *et al.*⁶

For this, 1.78 g $\text{ZrOCl}_2 \times x\text{H}_2\text{O}$ were dissolved in 40 mL MilliQ water, a diffusive gel was added and the volume topped up to 100 mL. The gel was soaked for at least 2 hours, retrieved, rinsed with MilliQ water, put into 100 mL MES buffer (0.05 M, pH 6.7) and placed for 40 minutes on a shaker. Zirconium oxide precipitation started immediately, resulting in a gel densely impregnated with Zr-oxide. The gel was retrieved, rinsed with MilliQ water and stored in a 0.01 M NaNO_3 solution until further use.

Agl binding gels for densitometric sulphide mapping. For densitometric sulphide analysis, we modified the sulphide binding gels described in Teasdale *et al.*⁷ by replacing the polyacrylamide gel matrix with Hydromed D4. The novel sulphide gels were produced by dispersing 1.25 g of the AgI slurry in 7.5 g 10% w/w D4 (ethanol : water, 9:1 w/w) solution using an Ultra-Turrax disperser. This cocktail was then knife-coated onto a dust-free Mylar PET foil using a 0.25 mm spacer. This novel procedure avoided handling of carcinogenic acrylamide and resulted in a more homogeneous AgI distribution than in the older method.⁷

Zr-oxide-SPR-IDA gels for anion-cation mapping using LA-ICPMS. Gels for simultaneous anion and cation binding were prepared according to Kreuzeder *et al.*⁸ Briefly, Zr-oxide was precipitated by slowly titrating a 30 g L^{-1} $\text{ZrOCl}_2 \times x\text{H}_2\text{O}$ solution with 0.1 mol L^{-1} NaOH until the pH stabilized at pH 7.0. The precipitate was washed and the water removed using a Buechner funnel. A D4 solution was prepared by dissolving 10 g of D4 in 100 mL of a 9:1 v/v ethanol-water solution. 15 g of the Zr-oxide slurry were added to a plastic vial and topped up to 100 mL with the D4 solution. The mixture was homogenized using an Ultra-Turrax disperser. Afterwards, 1 mL of SPR-IDA suspension was added to 9 mL of the Zr-oxide solution and mixed vigorously by hand. Air bubbles were removed by rotating the vial slowly in an overhead shaker overnight. Subsequently, three layers of this solution were knife-coated onto a glass plate on top of each other, allowing for evaporation of the solvent in an oven between coating the individual layers. The glass plate was immersed in MilliQ for at least 4 h for gel hydration. After this period, the gel detached easily from the glass. The gel was fully hydrated for another 24 h and was then stored in a 10 mmol L^{-1} NaNO_3 solution at 6°C.

(g) DGT gel analysis and image generation - gel-based rhizospheric sulphide, phosphate, Fe(II) and Ca²⁺ determination

Single-element mapping of sulphide and phosphate.

Molybdate-blue staining of the precipitated Zr-oxide gels. After deployment and phosphate sampling in the sediment, the Zr-oxide gels were subjected to the densitometric phosphate mapping method described by Ding *et al.*⁹ with slight modifications. Due to time restrictions at the field station, phosphate immobilization by heating the retrieved gels to 85 °C was only done for 12 h instead of 5 days, however this period is sufficient to largely avoid solubilisation of sampled P into the acidic staining solution.⁹ The color development step was conducted at room temperature (30 °C) instead of 35°C. Afterwards, the precipitated Zr-oxide gels were immersed in a molybdate blue staining reagent for 45 min.⁹ This procedure led to blue color formation at gel locations where phosphate was bound. Subsequently, the stained Zr-oxide gels were subjected to computer imaging densitometric (CID) analysis.

Computer imaging densitometry of the AgI and precipitated Zr-oxide gels. Analyte-sensitive gels (precipitated Zr-oxide gels for phosphate and AgI gels for sulphide) were deployed into the experimental microcosms for 12 h, and subjected to computer imaging densitometric (CID) analysis. This analysis was conducted using a printer with incorporated flatbed scanner (Canon MG2460, Canon, Japan) according to published procedures.^{7,9} After retrieval of the gels, the protective mesh was removed. The precipitated Zr-oxide gels were stained as described above. The AgI gels were left untreated, utilizing the contrast of the formed black Ag₂S against the pale white background of the AgI gel at locations where no sulphide was bound.⁷ The retrieved sulphide and phosphate sensitive gels were then fixed flat between two transparent PET sheets in order to avoid direct contact with the scanner, scanned at a resolution of 600 dpi and saved as color and greyscale .tiff files. For calibration, standard gels were exposed to known analyte concentrations, subsequently stained (only accounts for the phosphorous sensitive gels) and scanned using the same scanner settings. From the obtained grayscale values and the known analyte concentrations, calibrations functions were determined using ImageJ (readout of grayscale values) and Origin Pro (data analysis and fitting) (OriginLab Corp., USA). Applied calibration curves are provided below (Fig. S5 & S6). The experimental sample gels were then analyzed based on the acquired calibration functions.

Laser ablation inductively coupled plasma mass spectrometric (LA-ICPMS) analysis

LA-ICPMS analysis was performed following Kreuzeder *et al.*⁸ Zr-oxide-SPR-IDA gels for simultaneous sampling of phosphate, Fe(II) and Ca²⁺ were deployed into the experimental mesocosms for 24 h. After deployment to the microcosms, the retrieved Zr-oxide-SPR-IDA gels were transferred to a piece of polyethersulphone (SUPOR, Pall corporation) membrane and dried using a gel dryer (Unigeldryer 3545, Laborgeräte and Vertriebs GmbH), resulting in an inseparable composite of the membrane and the dried gel.⁸ These composites were then mounted on glass slides using double-sided adhesive tape and subjected to LA-ICPMS analysis on a UP 193-FX (ESI, NWR division) laser ablation instrument coupled to a Nexion 350D ICPMS (Perkin Elmer) in line-scanning mode using the following parameters: inter-line distance: 400 µm, laser spot size diameter: 150 µm, line scanning speed: 250 µm s⁻¹, laser pulse frequency: 20 Hz, irradiance: 1-2 J cm⁻². Argon was used as the carrier gas. Count rates were recorded for several isotopes including ¹³C, ³¹P, ⁴⁴Ca and ⁵⁷Fe, where ¹³C was used as internal normalisation standard. Total ICPMS measurement cycle times were 0.383 and 0.453 s for two individual measurement days. These settings resulted in horizontal spatial resolutions of 96 µm (Fig. 3, dark; Fig. S9, light) and 113 µm (Fig. 3 light; Fig. S9, dark), and a vertical spatial resolution of 400 µm. Chemical images were generated and arranged using Microsoft Excel (Microsoft Corp., Redmond, USA), ImageJ, Systat SigmaPlot (Systat Software Inc., San Jose, USA), Adobe Photoshop and Adobe InDesign (Adobe Corp., San Jose, USA).

(h) DGT interpretation

While planar optodes provide a direct concentration measurement, the DGT measurement cannot be directly interpreted as an actual porewater concentration. DGT gels continuously bind analytes from the exterior solution during deployment. After gel retrieval and fixation, LA-ICPMS and CID quantify the mass of analyte taken up by the gel as a surface concentration c_s , *e.g.* in µg cm⁻². Due to the well-defined sampling geometry, this parameter can be converted to the concentration at the sampler-exterior solution interface, c_{DGT} , as:¹⁰

$$c_{DGT} = c_s \frac{\Delta g}{Dt}$$

where Δg is the thickness of the diffusion layer overlying the binding gel (in this study: Nuclepore membrane and plankton mesh, respectively), D is the analyte diffusion coefficient inside the diffusion layer⁷ (DGT Research Ltd at <http://www.dgtresearch.com/diffusion-coefficients>, last visited 09 June 2016), and t is the deployment time. As c_{DGT} is calculated from the mass of analyte

accumulated during the total gel deployment time, it represents the time-averaged analyte concentration at the sampler-solution interface.

In simple, synthetic aqueous solutions containing only fully labile analyte species, c_{DGT} provides a direct measure of the exterior solution concentration, as the flux of analyte to the DGT gel is constant throughout the deployment time. In sediments, the porewater concentration of many solutes is governed by sorption/desorption and dissolution/precipitation equilibria, so solutes are usually not fully labile.¹¹ Sediment tortuosity further restricts solute diffusivity. Therefore, DGT analytes are depleted in sediment adjacent to the sampler as a consequence of being sequestered by the binding gel. The actual porewater concentration at the sampler-sediment interface is thus decreasing progressively during sampling, as is the flux into the DGT sampler. The c_{DGT} concentration obtained under these circumstances is therefore smaller than the porewater concentration without perturbation by DGT sampling.^{11,12}

(i) Calibration plots

Planar optode calibrations

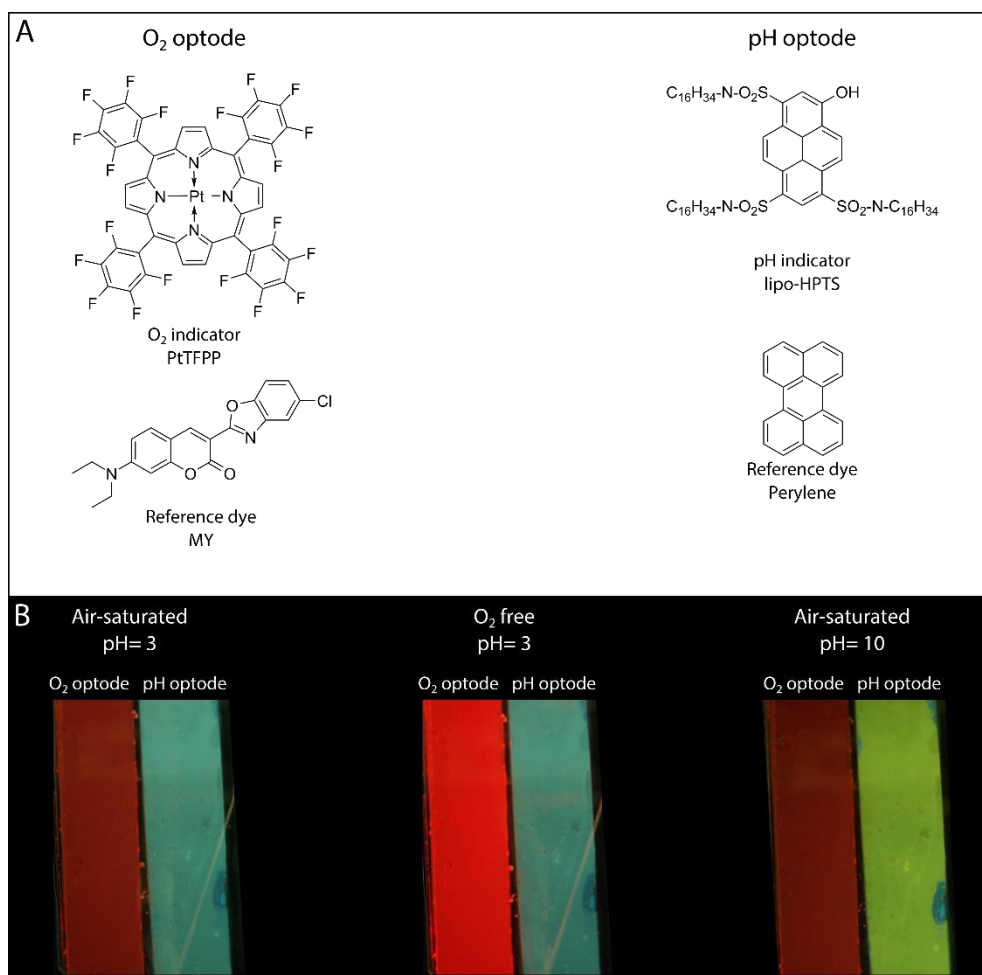


Figure S3. (A) Chemical structures of the indicators and reference dyes used in the O₂ and pH optodes, respectively. (B) Images of an O₂ and pH optode positioned next to each other and exposed to different analyte concentrations. The images were obtained with a SLR camera (EOS 1000D, Canon, Japan) and the optodes were excited using a hand-held UV lamp. In this setup, the O₂ sensor had no additional optical isolation layer.

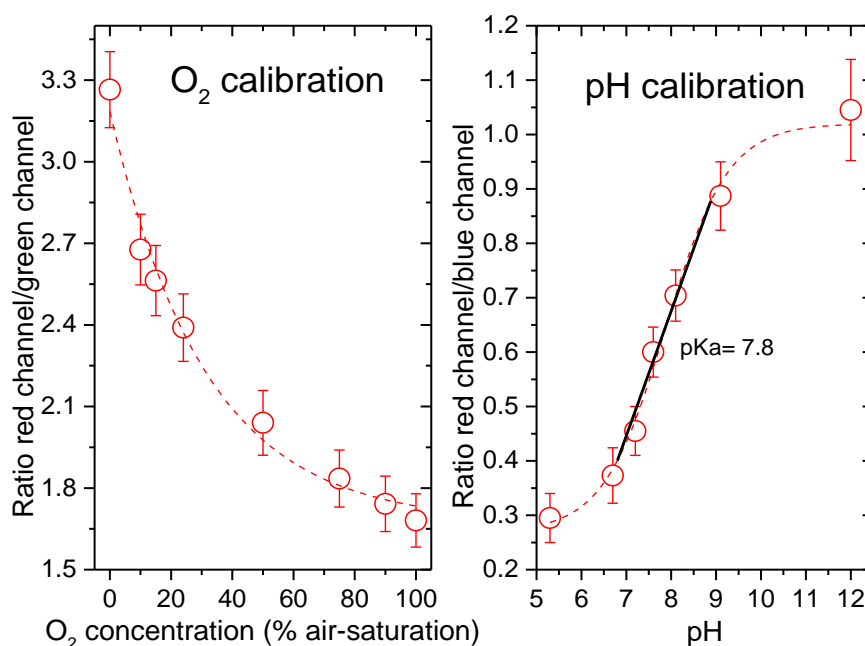


Figure S4. Calibration plots of the O₂ and pH optodes used in the study. Symbols with error bars represent means \pm standard deviation ($n=3-6$). For the O₂ optode, a single exponential decay function was fitted to the calibration measurements (dashed line; $R^2 > 0.98$) and this fit was used for calibrating the experimental O₂ images. The pH optode response was fitted using a sigmoidal function (dashed line; $R^2 > 0.98$). For practical reasons, a linear fit in the range $pK_a \pm 1$ was used (depicted as the black line in the calibration plot). Within the chosen range (pH 7-9) this type of linear fit describes the sensor response to changing pH values very well ($R^2 > 0.98$), without notable experimental errors.

DGT calibrations

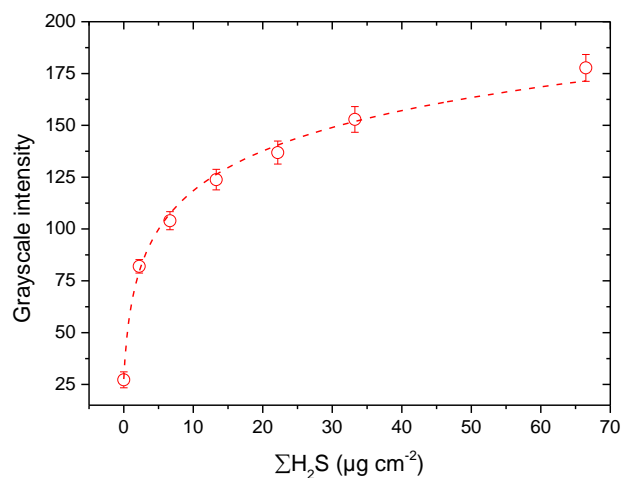


Figure S5. Calibration plot of the sulphide-binding AgI gel used in this study. All data points represent mean values \pm S.D. ($n=3-6$) and were fitted using the following function: $y=b*\ln(x-a)$; ($R^2 > 0.99$).

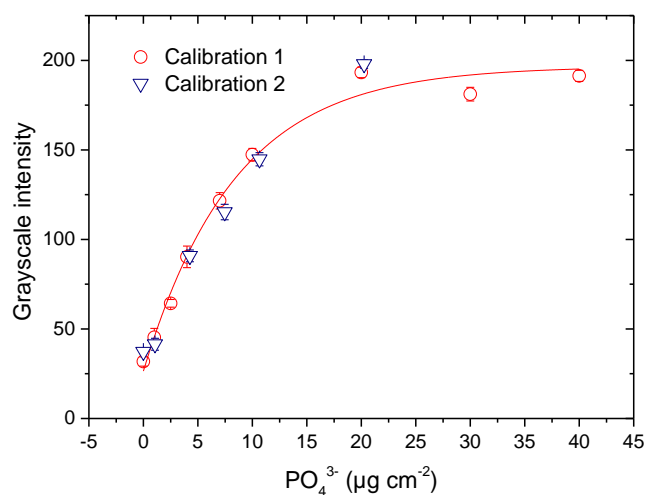


Figure S6. Calibration plot of the PO_4^{3-} binding precipitated Zr-oxide gel used in this study. The curve shows a calibration of gels made in Denmark and shipped to Australia (Calibration 1) and one of gels made at the remote study site (Green Island, Cairns, Australia; Calibration 2). Data points with error bars represent mean values \pm S.D. ($n=3-6$) and were fitted using the following function: $y=y_0 + A*e^{R0*x}$; ($R^2 > 0.98$).

SUPPLEMENTARY DATA AND TEXT

Figure S7.

O₂ distribution and dynamics in the seagrass rhizosphere

Specimen of the seagrass *Cymodocea serrulata* were leaking O₂ from the basal leaf meristem (upper arrow) and the root apical meristems (two lower arrows) into the immediate rhizosphere, with much higher radial O₂ loss (ROL) and larger oxenic microzones in the rhizosphere during light stimulation of the leaf canopy. Such seagrass-derived oxenic microzones can alter the sediment biogeochemistry providing micro-habitats for distinct microbial communities, such as sulphide-oxidizing bacteria, within the oxenic microniches and sulphate-reducing bacteria at the plant/sediment- and oxenic/anoxic interface¹³ (Brodersen et al. *unpublished data*). The ROL facilitates sediment detoxification via sulphide re-oxidation within the seagrass-derived oxenic microniches.¹⁴

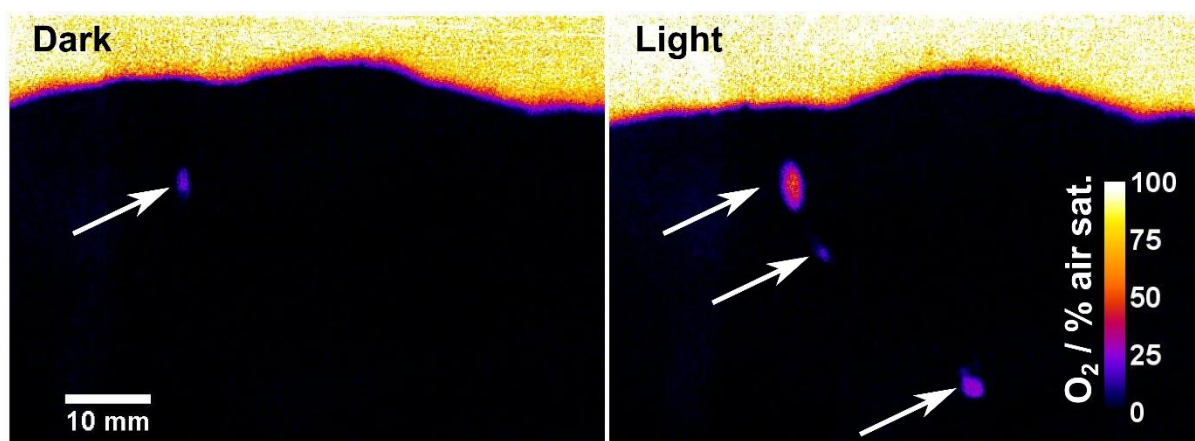


Figure S7. Distribution and dynamics of O₂ concentration within the rhizosphere of the tropical seagrass *Cymodocea serrulata*. Seagrasses were exposed to dark and light conditions (incident photon irradiance of $\sim 500 \mu\text{mol photons m}^{-2} \text{s}^{-1}$). Arrows indicate seagrass-derived oxenic microzones. The color bar depicts the O₂ concentration in % air saturation. The seagrasses were transplanted into sieved (<1 mm sediment fraction) natural sediment from the sampling site to exclude any larger animals and bivalves, as well as to ensure natural ratios of essential nutrients and rhizosphere microbes.

Figure S8*pH heterogeneity and dynamics within the seagrass rhizosphere*

Pronounced spatio-temporal pH heterogeneity and dynamics was observed in the rhizosphere of *Cymodocea serrulata*, exhibiting several microniches of low pH especially around the root apical meristems (*i.e.* the root-caps), the root/shoot junctions, and the basal leaf meristem. These observations correlated well with the O₂ concentration images revealing radial O₂ loss (ROL) from these specific regions of the plant (Fig. S7). Light stimulation of the leaf canopy induced photosynthetic O₂ evolution in the seagrass leaves driving an enhanced internal O₂ concentration gradient and higher ROL to the rhizosphere, where enhanced sulphide oxidation resulted in lower rhizosphere pH levels around roots and root/shoot junctions.

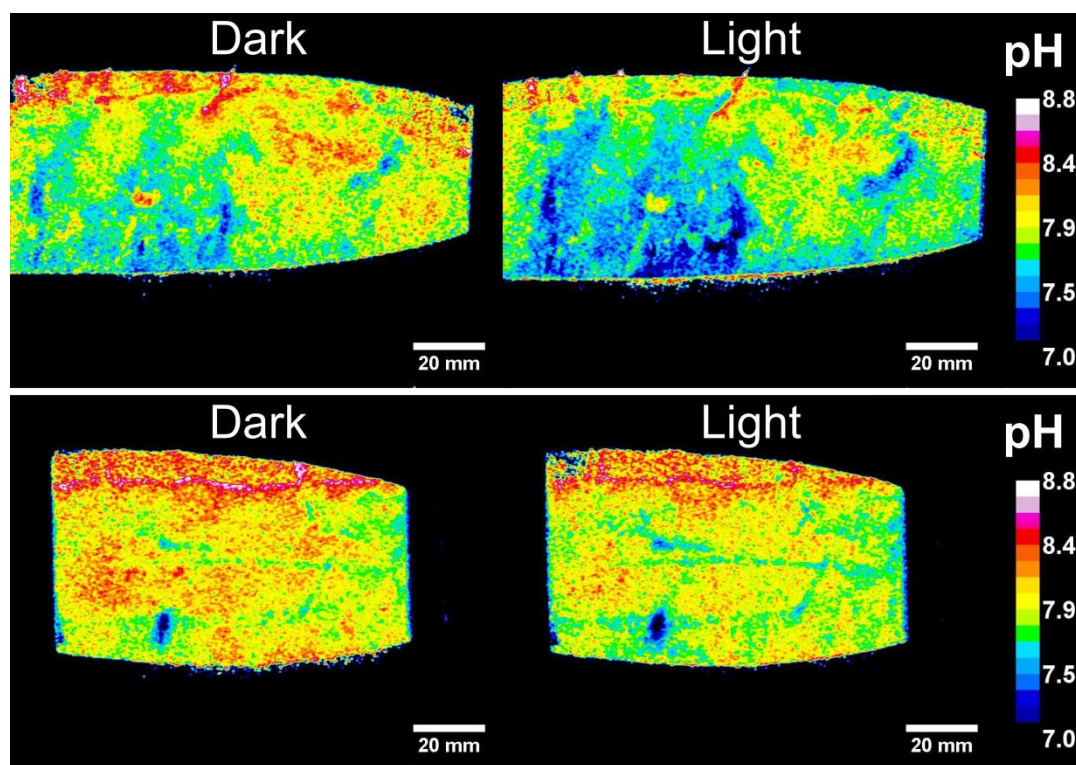


Figure S8. pH heterogeneity and dynamics within the seagrass rhizosphere of two specimens of the tropical seagrass *Cymodocea serrulata* during dark and light conditions (incident photon irradiance of $\sim 500 \mu\text{mol photons m}^{-2} \text{s}^{-1}$). The color coding depicts the pH value. The seagrasses were transplanted into sieved ($<1 \text{ mm}$ sediment fraction) natural sediment from the sampling site to exclude larger animals and bivalves, as well as to ensure natural ratios of essential nutrients, buffering salts and microbes, respectively.

Figure S9*Combined chemical imaging of Fe(II), phosphate and pH*

Figure S9 shows the Fe(II), phosphate and pH distribution at the root/sediment interface during light and dark conditions. Higher concentrations of soluble Fe(II) and phosphorus were measured around the roots of the seagrass *Cymodocea serrulata* as compared to the surrounding sediment (Fig. S9a,c). Seagrass-generated low-pH microniches in the rhizosphere owing to radial O₂ loss (ROL) and probably organic acid release (Fig. S7-8) led to carbonate dissolution and subsequent phosphate release to the porewater around the root-tip of the 4th root (Fig. S9-10). We also found increased local sulphide production (Figure 2) leading to reduction of Fe(III)-oxyhydroxides to dissolved Fe(II) (Fig. S9a,c). Concomitantly, phosphate precipitated as Fe(III)-phosphate and adsorbed onto Fe(III)-oxyhydroxides was released to the porewater.

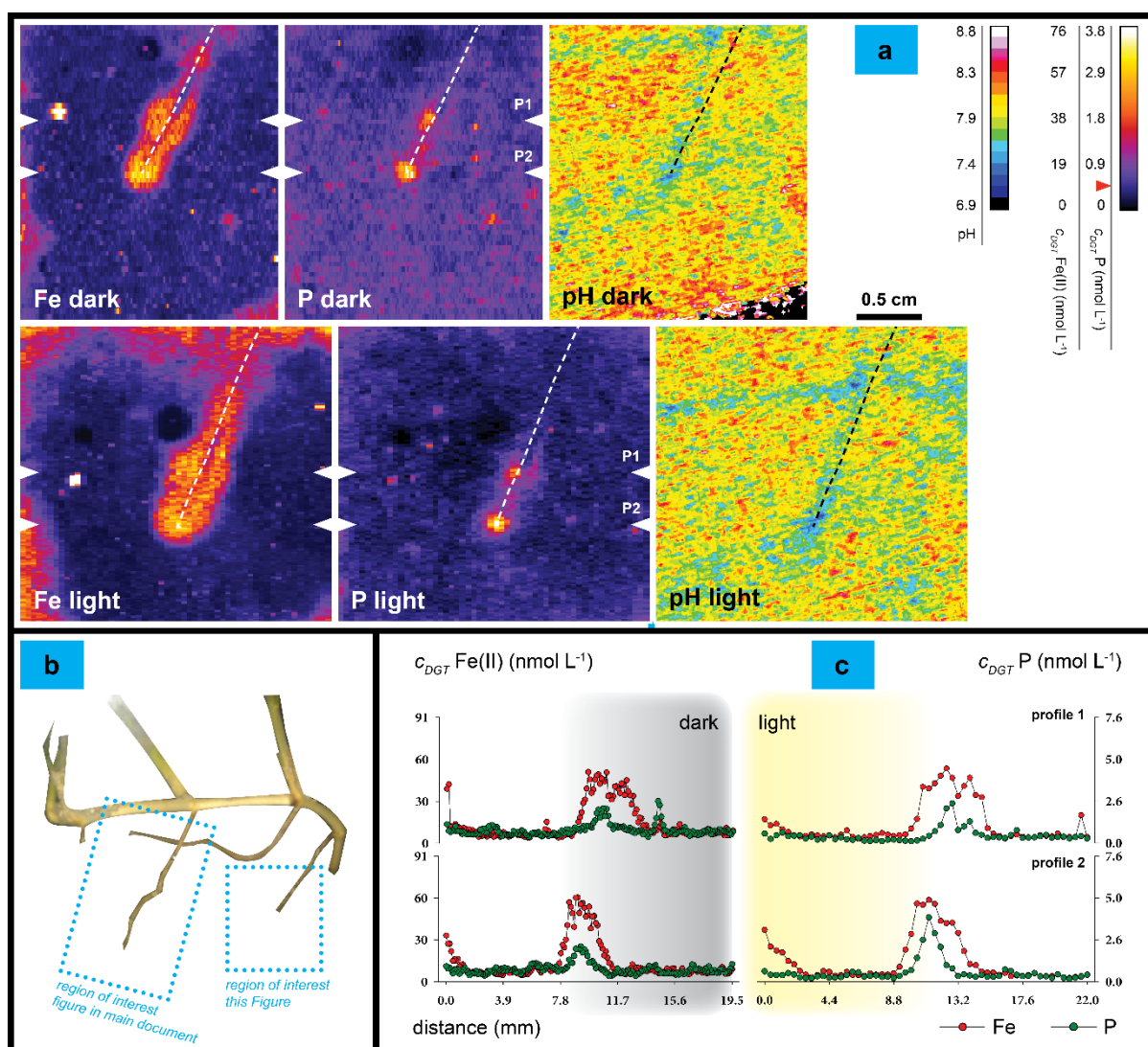


Figure S9. Fe(II), phosphorus and pH distribution in the rhizosphere of the tropical seagrass species *Cymodocea serrulata* during dark and light conditions (incident photon irradiance of $\sim 500 \mu\text{mol photons m}^{-2} \text{ s}^{-1}$) (a,c). All images were color coded, where the color scales depict the sediment pH, Fe(II) and phosphorus concentrations, respectively. The dotted lines in the chemical images show the position of the roots (a). The red arrow on the phosphate calibration bar denotes the method detection limit (MDL) of the LA-ICPMS measurement. No such arrow is shown for Fe as the MDL was negligibly small in this case. Marked areas in panel (b) depict the selected regions of interest within the seagrass rhizosphere as visualized in the color coded chemical images (panel a; and on Figure 4 in the main text). Note the different scale on the y-axis (c).

Figure S10

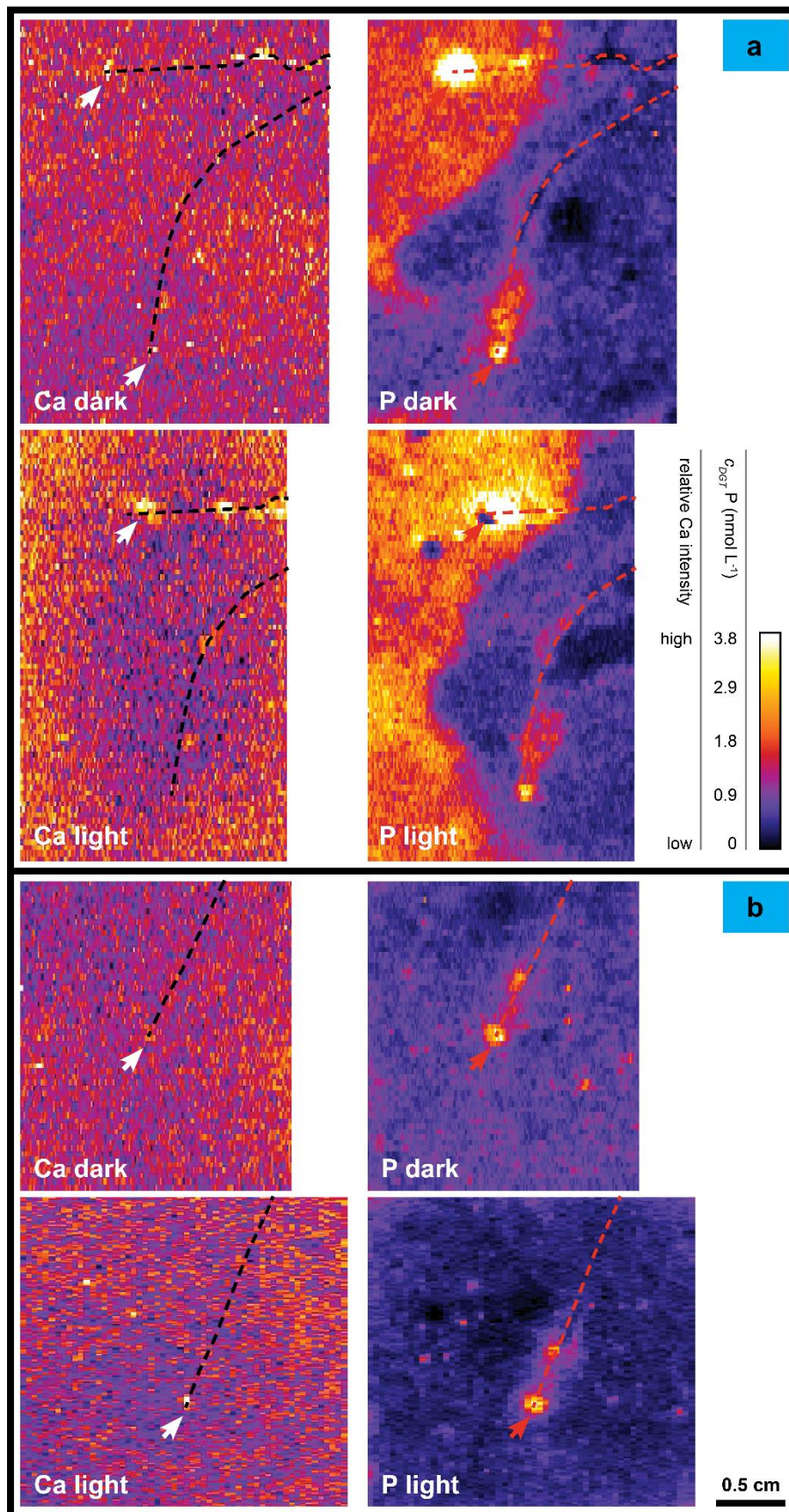


Figure S10. Distribution and dynamics of calcium (Ca) within the rhizosphere of the tropical seagrass *Cymodocea serrulata*. Seagrasses were exposed to dark and light conditions (incident photon irradiance of $\sim 500 \mu\text{mol photons m}^{-2} \text{s}^{-1}$). The color bar depicts the relative Ca intensity. The dotted lines on the chemical images show the position of the roots. (a) Shows the Ca distribution around the 2nd and 3rd roots, while (b) shows the Ca distribution around the 4th root. Red and white arrows mark co-localized, rhizosphere Ca and phosphorus (P) hotspots. The seagrasses were transplanted into sieved (<1 mm sediment fraction) natural sediment from the sampling site to exclude any larger animals and bivalves, as well as to ensure natural ratios of essential nutrients and rhizosphere microbes.

References

- (1) Borisov, S. M.; Herrod, D. L.; Klimant, I. Fluorescent poly(styrene-block-vinylpyrrolidone) nanobeads for optical sensing of pH. *Sensors and Actuators B: Chemical* **2009**, 139, 52–58.
- (2) Ralph, P. J.; Short, F. T. Impact of the wasting disease pathogen, *Labyrinthula zosterae*, on the photobiology of eelgrass *Zostera marina*. *Marine Ecology Progress Series* **2002**, 226, 265–271.
- (3) Larsen, M.; Borisov, S. M.; Grunwald, B.; Klimant, I.; Glud, R. N. A simple and inexpensive high resolution color ratiometric planar optode imaging approach: application to oxygen and pH sensing. *Limnology and Oceanography: Methods* **2011**, 9, 348–360.
- (4) Mosshammer, M.; Strobl, M.; Köhl, M.; Klimant, I.; Borisov, S. M.; Koren, K. Design and application of an optical sensor for simultaneous imaging of pH and dissolved O₂ with low cross-talk. *ACS Sensors* **2016**, accsensors.6b00071.
- (5) Zhang, H.; Davison, W. Diffusional characteristics of hydrogels used in DGT and DET techniques. *Anal Chim Acta* **1999**, 398, 329–340.
- (6) Guan, D.; Williams, P. N.; Luo, J.; Zheng, J.; Xu, H.; Cai, C.; Ma, L. Q. Novel Precipitated Zirconia-Based DGT Technique for High- Resolution Imaging of Oxyanions in Waters and Sediments. *Environ Sci Technol* **2015**, 49, 3653-3661.
- (7) Teasdale, P. R.; Hayward, S.; Davison, W. In situ, High-Resolution Measurement of Dissolved Sulfide Using Diffusive Gradients in Thin Films with Computer-Imaging Densitometry. *Analytical chemistry* **1999**, 71, 2186–2191.
- (8) Kreuzeder, A.; Santner, J.; Prohaska, T.; Wenzel, W. W. Gel for simultaneous chemical imaging of anionic and cationic solutes using diffusive gradients in thin films. *Analytical Chemistry* **2013**, 85, 12028–12036.
- (9) Ding, S.; Wang, Y.; Xu, D.; Zhu, C.; Zhang, C. Gel-based coloration technique for the submillimeter-scale imaging of labile phosphorus in sediments and soils with diffusive gradients in thin films. *Environmental Science and Technology* **2013**, 47, 7821–7829.
- (10) Davison, W.; Zhang, H. In situ speciation measurements of trace components in natural waters using thin-film gels. *Nature* **1994**, 367, 546–548.
- (11) Davison, W.; Zhang, H.; Warnken, K. W. Chapter 16 Theory and applications of DGT measurements in soils and sediments. *Comprehensive Analytical Chemistry* **2007**, 48, 353–378.
- (12) Santner, J.; Larsen, M.; Kreuzeder, A.; Glud, R. N. Two decades of chemical imaging of solutes in sediments and soils – a review. *Analytica Chimica Acta* **2015**, 878, 9-42.
- (13) Jensen, S. I.; Köhl, M.; Priemé, A. Different bacterial communities associated with the roots and bulk sediment of the seagrass *Zostera marina*. *FEMS Microbiology Ecology* **2007**, 62, 108–117.
- (14) Brodersen, K. E.; Nielsen, D. A.; Ralph, P. J.; Köhl, M. Oxidic microshield and local pH enhancement protects *Zostera muelleri* from sediment derived hydrogen sulphide. *New Phytologist* **2015**, 205, 1264–1276.